Title: The Anthropocene is functionally and stratigraphically distinct from the Holocene

Authors: Colin N. Waters,[1]* Jan Zalasiewicz,[2] Colin Summerhayes,[3] Anthony D. Barnosky,[4] Clément Poirier,[5] Agnieszka Gałuszka,[6] Alejandro Cearreta, [7] Matt Edgeworth, [8] Erle C. Ellis, [9] Michael Ellis, [1] Catherine Jeandel, [10] Reinhold Leinfelder, [11] J.R. McNeill, [12] Daniel deB. Richter, [13] Will Steffen, [14] James Syvitski, [15] Davor Vidas, [16] Michael Wagreich, [17] Mark Williams, [2] An Zhisheng, [18] Jacques Grinevald, [19] Eric Odada, [20], Naomi Oreskes, [21] and Alexander P. Wolfe, [22].

Affiliations: [1]British Geological Survey, Keyworth, Nottingham NG12 5GG, UK.
[2]Department of Geology, University of Leicester, University Road, Leicester LE1 7RH, UK.
[3]Scott Polar Research Institute, Cambridge University, Lensfield Road, Cambridge CB2 1ER, UK.
[4]Dept. of Integrative Biology, Museum of Paleontology, Museum of Vertebrate Zoology, University of California, Berkeley, CA 94720, USA.
[5]Morphodynamique Continentale et Côtière, Université de Caen Basse Normandie, CNRS; 24 rue des Tilleuls, F-14000 Caen, France.
[6]Geochemistry and the Environment Division, Institute of Chemistry, Jan Kochanowski University, 15G Świętokrzyska St, 25-406 Kielce, Poland.
[7]Departamento de Estratigrafía y Paleontología, Facultad de Ciencia y Tecnología, Universidad del País Vasco UPV/EHU, Apartado 644, 48080 Bilbao, Spain.
[8]School of Archaeology and Ancient History, University of Leicester, University Road, Leicester LE1 7RH, UK.
[9]Department of Geography and Environmental Systems, University of Maryland Baltimore County, Baltimore MD 21250, USA.
[10]LEGOS (CNRS/CNES/IRD/Université Paul Sabatier), 14 avenue Edouard Belin, 31400 Toulouse, France.
[11]Department of Geological Sciences, Freie Universität Berlin, Malteserstr. 74-100/D, 12249 Berlin, Germany.
[12]Georgetown University, Washington DC, USA.
[13]Nicholas School of the Environment Duke University, Box 90233, Durham, North Carolina, 27516, USA.
[14]The Australian National University, Canberra ACT 0200, Australia.
[15]University of Colorado-Boulder Campus, Box 545, Boulder CO, 80309-0545, USA.
[16]Marine Affairs and Law of the Sea Programme, The Fridtjof Nansen Institute, Norway.
[17]Department of Geodynamics and Sedimentology, University of Vienna, A-1090 Vienna, Austria.
[18] State Key Laboratory of Loess and Quaternary Geology, Institute of Earth Environment, Chinese Academy of Sciences, Xi'an 710061, China.
[19]IHEID, Chemin Eugène Rigot 2, 1211 Genève 11 Switzerland.
[20]Department of Geology, University of Nairobi, Kenya.
[21]Department of the History of Science, Harvard University, Cambridge, MA 02138, USA.
[22]Department of Biological Sciences, University of Alberta, Edmonton, AB T6G 2E9, Canada

*Corresponding author. E-mail: cnw@bgs.ac.uk

BACKGROUND: Humans are altering the planet at an increasing rate, including long-term, global geologic processes. Any formal recognition of an Anthropocene Epoch in the geological time scale hinges on whether humans have changed the Earth system sufficiently to produce a stratigraphic signature in sediments and ice distinct from that of the Holocene Epoch.Proposals for recognizing the start of the Anthropocene include an 'early Anthropocene' reflecting spread of agriculture and deforestation; Columbian Exchange of Old World and New World species; the Industrial Revolution at ~1800; and the mid-twentieth century 'Great Acceleration' of population growth and industrialization.

ADVANCES: Recent anthropogenic deposits contain new minerals and rock types, with rapid global dissemination of novel materials including elemental aluminum, concrete and plastics, shaped into abundant rapidly-evolving 'technofossils'. Fossil-fuel combustion has disseminated black carbon, inorganic ash spheres and spherical carbonaceous particles worldwide, showing near-synchronous global increase around 1950. Anthropogenic sedimentary flux changes have intensified, including enhanced erosion through deforestation and road construction. Widespread sediment retention behind dams has amplified substantive delta subsidence.

Geochemical signatures include elevated levels of polyaromatic hydrocarbons, polychlorinated biphenyls and pesticide residues, and increased $^{207/206}$Pb ratios from leaded gasoline, largely from ~1945–50. Soil nitrogen and phosphorus inventories have doubled in the past century through increased fertilizer use, generating widespread signatures in lake strata and nitrate levels in Greenland ice higher than any time during the previous 100,000 years.

Detonation of the Trinity atomic device at Alamogordo New Mexico on July 16, 1945 initiated local nuclear fallout from 1945–1951, whereas thermonuclear weapons tests generated a clear global signal from 1952 as a 'bomb spike' of excess ^{14}C, ^{239}Pu and other artificial radionuclides.

Atmospheric CO_2 and CH_4 concentrations depart from Holocene and indeed Quaternary patterns from ~1850, markedly from ~1950, with associated steep fall in δ^{13}C permanently captured by tree-rings and calcareous fossils. An average global temperature increase of 0.6-0.9^{o}C from 1900, mostly in the last 50 years, is now rising beyond the Holocene variation of the last 1400 years, along with modest enrichment of δ^{18}O in Greenland ice from ~1900. Global sea-levels increased at 3.2 ± 0.4 mm/year from 1993-2010, and are now rising above Late Holocene rates. Depending on the trajectory of future anthropogenic forcing, these trends may reach or exceed the envelope of Quaternary interglacial conditions.

Biologic changes have not produced signatures of global change as sharp as those of compared to chemical and physical processes. Yet biotic extinction rates, far above background since 1500, increased further in the 19th century and later, while species assemblages have altered worldwide due to geologically unprecedented trans-global species invasions and changes associated with farming and fishing, permanently reconfiguring Earth's biological trajectory.

OUTLOOK: These novel stratigraphic signatures support formalization of the Anthropocene at the epoch level, with a lower boundary (still to be formally identified) suitably placed in the mid-20th century. Formalization is a complex question as - unlike with prior

subdivisions of geological time - potential utility of a formal Anthropocene reaches well beyond the geological community. It also expresses the extent to which humanity is driving rapid and widespread changes to the Earth system that will variously persist and potentially intensify into the future.

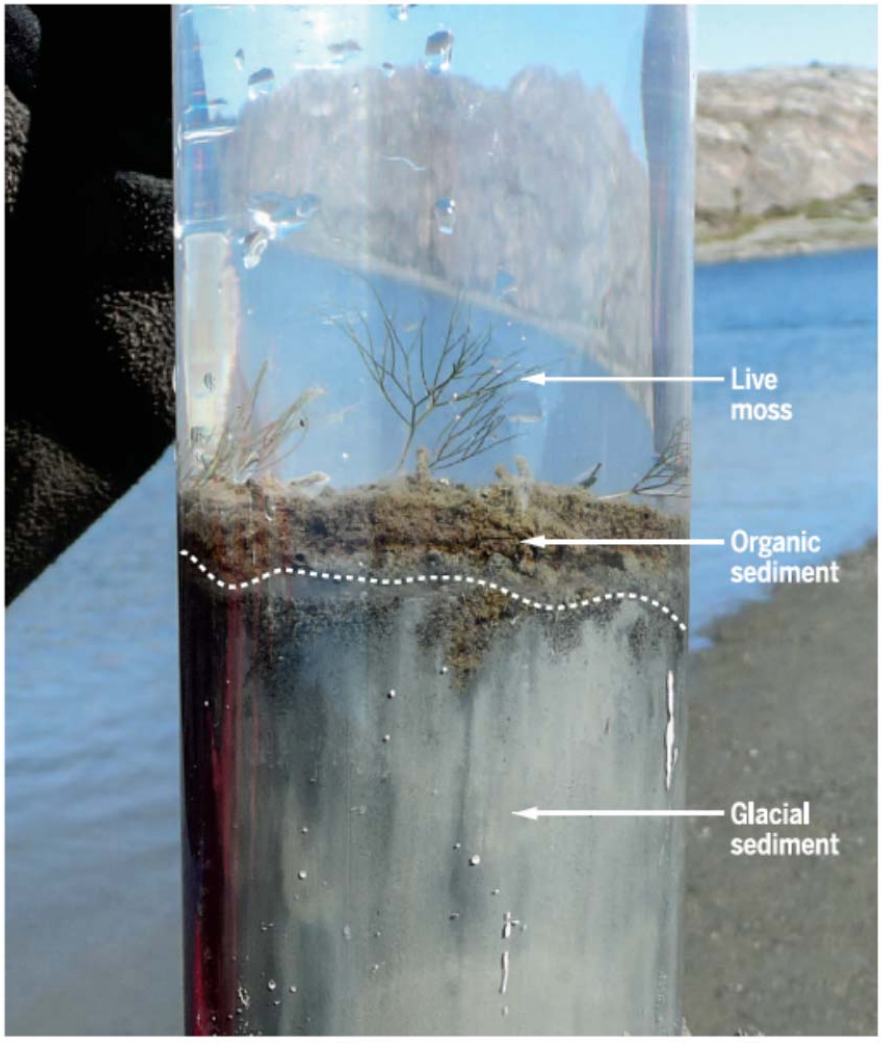

Indicators of the Anthropocene in recent lake sediments differ markedly from Holocene signatures. These include unprecedented combinations of plastics, fly ash, radionuclides, metals, pesticides, reactive nitrogen and consequences of increasing greenhouse gas concentrations. Here, in west Greenland (69˚03'N, 49˚54'W), glacier retreat due to climate warming has resulted in abrupt stratigraphic transition from proglacial sediments to non-glacial organic matter, effectively demarcating the onset of the Anthropocene (Photo credit: J.P. Briner).

Abstract:

Human activity is leaving a pervasive and persistent signature on Earth. Vigorous debate continues about whether this warrants recognition as a new geologic time unit known as the Anthropocene. We review anthropogenic markers of functional changes in the Earth system through the stratigraphic record. The appearance of manufactured materials in sediments − including aluminum, plastics and concrete − coincides with global spikes in fallout radionuclides and particulates from fossil-fuel combustion. Carbon, nitrogen, and phosphorus cycles have been substantially modified over the last century. Rates of sea-level rise, and the extent of human perturbation of the climate system, exceed Late Holocene changes. Biotic changes include species invasions worldwide and accelerating rates of extinction. These combined signals render the Anthropocene stratigraphically distinct from the Holocene and earlier epochs.

Introduction

The term 'Anthropocene' is currently used informally to reflect different concepts, including geological, ecological, sociological and anthropological changes in recent Earth history. The origins of the concept of the Anthropocene, its terminology and its socio-political implications are widely discussed (*1, 2*). When considering the stratigraphic definition of the Anthropocene, there are two basic questions: Have humans changed the Earth system to such an extent that geological deposits forming now and in the recent past include a signature distinct from that of the Holocene and earlier epochs which will remain in the geological record? If so, when did the stratigraphic signal (not necessarily the first detectable anthropogenic change) become recognizable worldwide? These questions are considered here in the context of how stratigraphic units have been formally recognized earlier in the Quaternary Period.

Proposals for recognizing the start of the Anthropocene have included: an 'early Anthropocene' reflecting the advent of agriculture, animal domestication, extensive deforestation and gradual increases in atmospheric carbon dioxide (CO_2) and methane (CH_4) levels thousands of years ago (*3, 4*); the Columbian Exchange of Old World and New World species following colonization of the Americas (*5*); the beginning of the Industrial Revolution at ~1800 C.E. (*6, 7*); and the mid-twentieth century 'Great Acceleration' of population growth, industrialization, mineral and energy use (*8-10*).

Here we review several lines of evidence which suggest that Anthropocene stratigraphic signatures distinguish it from the Holocene (Fig. 1). We find that criteria available to recognize the Anthropocene are consistent with those used to define other Quaternary stratigraphic units. Earlier Quaternary time unit subdivisions are defined by signals derived from climatic change cyclical forcings, such as variance in Earth's orbit, solar irradiance, or irregular events such as volcanic eruptions. Although these forcings continue, the Anthropocene markers derive from an additional key driver, that of human modification of global environments at unprecedented rates. That driver has produced a wide range of anthropogenic stratigraphic signals (Fig. 1), including examples that are novel in Earth history, global in extent and offer fine temporal resolution. The signals vary in their development: some are already advanced and others are at early stages. We describe these signals and suggest how they may be used in the stratigraphic

characterization and correlation of a formalized Anthropocene Epoch with a lower boundary (still to be identified) potentially placed in the mid-20th century.

How are Quaternary stratigraphic units defined?

The Quaternary Period, which began 2.6 million years ago (Ma), is subdivided into geochronological time units (epochs and ages), with boundaries linked at least in part to climate change events (expressed as Marine Isotope Stages), in association with paleomagnetic reversals (*11*). This contrasts with the subdivision of most of the Phanerozoic Eon (the last ~541 ± 1 Ma), for which the first or last appearance of key fossil taxa is typically used to define time units. Fossil-based boundaries represent change at rates too slow and time-transgressive for the geologically recent past, in which the time units are of comparatively short duration (about 12,000 years for the Holocene, versus 2 million years (Myr) or more for earlier epochs). These time intervals are recognizable as chronostratigraphic units (series and stages), which, in contrast to the time units, are physical entities—rocks, sediments and glacier ice. Ideally, the chronostratigraphic units are exemplified, and their lower boundary defined, at a single locality as a Global Boundary Stratotype Section and Point (GSSP), typically in marine strata for pre-Holocene series (*12*).

The start of the Holocene Epoch (or Series) is based upon the termination of the transition from the last glacial phase through an interval of warming accompanied by ~120 m of sea-level rise. The warming took place over about 1600 years and is recorded by a variety of stratigraphic signals that are not all globally synchronous. In the Northern Hemisphere, a signal suitable for pinpointing the Holocene's beginning was taken as the abrupt end of the 'Younger Dryas' cooling event. The GSSP chosen to define the base of the Holocene was agreed to lie within the NGRIP2 ice core from central Greenland (*13*). The core contains a detailed archive of environmental change, preserved in the composition of air bubbles trapped in the ice and in the chemical and physical characteristics of the ice. The GSSP lies within a multi-decade warming and moistening trend, inferred from oxygen isotopes showing rising $\delta^{18}O$, associated with a reduction in dust content. About midway on this trend, the sharpest change is a decrease in excess deuterium, interpreted as representing a reorganization of North Atlantic ocean-atmosphere circulation at 11,700 years before 2000 C.E. ± 99 years at 2 σ (*13*). This distinctive change is used to define the base of the Holocene Series (the material chronostratigraphic unit). Thus, by definition the Holocene Epoch—the abstract time unit—began ~11,700 years ago.

The Holocene Epoch (and corresponding Series) is being considered for subdivision into three component Sub-epochs (Sub-series), again using climatic signatures to guide the positioning of their bases. The base of the Lower Holocene, by default, is the base of the Holocene Series, as described above. The base of the Middle Holocene has been proposed to lie within a short-lived (150 ± 30 years) cooling event at 8,200 B.P., where there is a marked shift to low $^{18}O/^{16}O$ values (i.e. more negative $\delta^{18}O$) within the NGRIP1 ice core in the Greenland Ice Sheet (*13*). At the same time, Greenland ice cores show low deuterium/hydrogen (D/H) ratios, a decline in annual layer thickness, an atmospheric CH_4 minimum and a volcanic marker characterized by high fluoride content. Such signals have led to the proposal that a Greenland ice core should be used to define the Middle Holocene GSSP (*13*). Although such signals are most strongly evident at localities adjacent to the North Atlantic, they likely reflect a global signature because correlative signals are evident in lake sediments as changes in pollen assemblages and oxygen isotopes; in cave speleothems as isotopic signals reflecting changes in the intensity of the South American monsoon; in marine foraminiferal assemblages (species

compositions); and in an increased aridification around the Mediterranean that broadly coincides with the Mesolithic-Neolithic transition (*13*).

The base of the Upper Holocene has been proposed to occur at a mid/low-latitude aridification event at 4,200 B.P. (*13*). This appears to have coincided with cooling of the North Atlantic and tropical Pacific, the arrival of cooler and wetter conditions in Europe, and weakening of the Asian monsoon (*13*). The proposed stratotype is in a speleothem record from Mawmluh Cave in north-east India, taken at the mid-point of a two-stage shift of $\delta^{18}O$ values in calcite from initially more positive values to later more negative ones, which took ~375 years (*13*). Although there is no doubt that marked environmental perturbations occurred at both 8,200 and 4,200 B.P., most proxies subsequently recovered in a matter of centuries, implying these were temporally discrete paleoclimatic events, as opposed to truly novel states within the Earth system.

Human drivers of stratigraphic signatures

The human driving forces responsible for many of the anthropogenic signatures are a consequence of the three linked force multipliers: accelerated technological development, rapid growth of human population, and increased consumption of resources. These combined to result in increased use of metals and minerals, fossil-fuels, agricultural fertilizers, and increased transformation of land and near-shore marine ecosystems for human use. The net effect has been loss of natural biomes to agriculture, cities, roads and other human constructs, and replacement of wild animals and plants by domesticated species to meet growing demands for food. This increase in consumption of natural resources is closely linked to the growth of the human population. Anatomically modern *Homo sapiens* emerged ~200,000 ago *(14)*. By 12,000 B.P., approximating to the start of the Holocene, humans had colonized all of the continents, except Antarctica and the South Pacific islands, and reached a total population estimated at 2 million (*15, 16*). To this point human influence on the Earth system was small compared to what has happened since the mid-20th century; even so, human impacts contributed to the extinction of Pleistocene megafauna (*17*). The key signals used to recognize the start of the Holocene Epoch (see above) were not directly influenced by human forcing, a major distinction from the proposed Anthropocene Epoch.

Humans have had a growing stratigraphic influence throughout the Holocene Epoch as the global population gradually increased. It has been argued that ~8,000 years ago, with a global population estimated at less than 18 million (*15, 16*), the initiation of agricultural practices and forest clearances began to gradually increase atmospheric CO_2 levels (*3*). But it was not until ~1800 C.E. that the global population first reached 1 billion (*16*). Increased mechanization and the drive to urbanization during the Industrial Revolution, initially in Western Europe then slowly expanding globally (*18*), then facilitated more rapid population increase. Although this population growth is commonly thought to have increased exponentially through the 19th and 20th centuries (cf. *8, 9*), recent analyses (*15, 16*) suggest that it can be differentiated into a period of relatively slower growth from 1750−1940 C.E., and one of more rapid growth from 1950−2010 C.E. The inflection point at ~1950 C.E. coincides with the 'Great Acceleration' (*8,*

9), a prominent rise in economic activity and resource consumption that accounts for the marked mid-20th century upturns or inceptions in the anthropogenic signals detailed below.

New anthropogenic materials

Recent anthropogenic deposits - the products of mining, waste disposal (landfill), construction and urbanization *(19)* - contain the greatest expansion of new minerals since the Great Oxygenation Event at 2400 Ma (*20*), accompanied by many new forms of 'rock' in the broad sense of geological materials with the potential for long-term persistence. Over many millennia, humans have manufactured materials previously unknown on Earth, such as pottery, glass, bricks and copper alloys. Remains of these materials are present as a persistent and widespread geological signal that is markedly time-transgressive, reflecting the migration of peoples (*21*). By contrast, elemental aluminum, almost unknown in native form before the 19th century, has seen 98% of its cumulative global production of ~500 Tg since 1950 C.E. (*20, 22*; Fig. 2A). Concrete, invented by the Romans, became the primary building material from World War II (1939–1945 C.E.) onwards. The last 20 years (1995–2015) account for more than half the 500,000 Tg of concrete ever produced (*22, 23*; Fig. 2A), equivalent to ~1 kg m^{-2} of the planet surface. Concrete and aluminum are widely disseminated across terrestrial, particularly urban, settings.

Similarly, the manufacture of new organic polymers (plastics), initially developed in the early 1900's, rapidly grew from the 1950's to an annual production of about ~300 Tg in 2013 (*24*; Fig. 2A), comparable to the present human biomass. Plastics spread rapidly via rivers into lakes , and are now also widespread in both shallow and deep-water marine sediments as macroscopic fragments, and as virtually ubiquitous microplastic particles (microbeads, 'nurdles' and fibers; Fig. 2A; *25– 27*), which are dispersed by both physical and biological processes. The decay-resistance and chemistry of most plastics suggests they will leave identifiable fossil and geochemical records.

These and other new materials are commonly shaped into abundant artifacts with the capacity to be preserved in, and help date, future geological deposits. Analogous to biotic fossil remains, these so-called technofossils (*28*) provide annual to decadal stratigraphic resolution (*22, 19*), far greater than can be obtained from first and last appearances of fossil taxa, which have traditionally provided the most common means of correlating stratal sections (*29*).

Fossil fuel combustion disseminates unburned particles as black carbon (BC), inorganic ash spheres (IAS) and spherical carbonaceous particles (SCPs). BC increases markedly towards the end of the 19th century, and especially from ~1970 C.E., with a peak at 6.7 Tg/year in ~1990 C.E. (*30*; Fig. 2B). IAS, locally detectable in the stratigraphic record from the 16th century, shows increases across Britain, Scandinavia and North America from ~1835 to 1960 C.E. (*31*). SCPs, first recorded in various sites in the UK from 1830–1860 C.E., show near-synchronous global increase around 1950 C.E., with peak signatures from the 1960's–1990's (*32, 33*; Fig. 2B). BC, IAS and SCPs, being airborne particulates, leave a permanent marker within both sediments and glacial ice. An ancient analogue, is the carbon impact spherules marker horizons at the Cretaceous–Paleogene boundary following the Chicxulub bolide impact (*34*). These low temperature natural spherules, readily distinguishable from high temperature industrial SCPs, demonstrate the likely persistence of SCPs as a stratigraphic marker (*32*).

Modification of sedimentary processes

The transformation of more than 50% of the land surface for human use (*35*) has generated anthropogenically modified materials that extend across multiple terrestrial settings. They are most ubiquitous in anthropogenic (artificial) deposits such as landfills, urban structures, and mine tailings, in addition to soils associated with cultivation. This influence is increasingly extending into the oceans, both directly, through coastal reclamation works, sediment reworking through trawler fishing, extraction of sand and gravel, and also indirectly, through changes in coastal sedimentary facies in response to rising sea levels, in the eutrophication of coastal environments, and via coral bleaching events *(36)*. Human land alteration also increasingly extends into the subsurface, with drilling into the Earth's crust to extract minerals, to store wastes, or to host utilities *(37)*. Mineral extraction alone accounts for the displacement of ~57,000 Tg/year of sediments, exceeding the current rate of river-borne sediment transport by almost a factor of 3 (*38*).

Human activities have also modified sedimentary processes sufficiently to leave clear expressions in river, lake, windblown and glacial deposits often far-removed from direct point sources *(36)*. Sediment fluxes in many fluvial systems increased through greater deforestation, livestock grazing and cropland development. Clearing of primary forests for agriculture, usually by burning, began in Early- to Mid-Holocene times, especially in temperate woodland biomes, shifting diverse primary forest communities towards domesticates and early successional species, and leaving widespread, time-transgressive, geological traces that include profound shifts in plant and animal remains, charcoal, and sediment deposits from soil erosion (*39, 40*). In recent decades, secondary forests have recovered across much of the temperate zone, and forest clearing has shifted towards tropical regions, for example with periods of rapid deforestation in Amazonia, Indonesia, and other regions in Asia and Africa in response to economic and governance dynamics (*41*). The construction of mountain roads in these tropical regions is resulting in substantial surface erosion and landslides *(42)*.

Extensive sediment retention behind dams constructed across major river systems has formed a more rapid global signal. Most dams were built in the past 60 years, at an average of more than one large dam per day (*8, 9*), and each will last 50 to 200 years, interrupting sediment transport to the oceans. The reduced sediment flux to major deltas, combined with increasing extraction of groundwater, hydrocarbons and sediments (for aggregates), has caused many large deltas to subside, a process beginning in the 1930's (*43*) at rates faster than modern eustatic sea-level rise (see below). Coastal retreat is an inevitable result. These various signals, abrupt on geological time scales, are diachronous at a decadal scale.

Changed geochemical signatures in recent sediments and ice

Anthropogenic materials and the human influence on sedimentary environments have near-global expression, but geochemical signatures − particularly those with airborne transport pathways − reach all global environments, including the ~12% of the Earth's surface permanently covered by ice. Among the many distinct geochemical signatures that human activities have introduced into the sedimentary record are elevated concentrations of polyaromatic hydrocarbons (PAHs), polychlorinated biphenyls (PCBs) and diverse pesticide residues, each beginning ~1945–1950 C.E. (*44-47*). Lead smelting during Roman times resulted in a distinctive local marker of increased $^{207/206}$Pb ratios, a signal that became evident globally

from the early 20th century as a result of vehicles powered by leaded gasoline (*47*). This illustrates that some geochemical signatures may vary in first appearance geographically, but nevertheless become useful as global markers when they rapidly spread as the result of new technologies in the mid-20th century.

Nitrogen (N) and phosphorus (P) in soils have doubled in the past century through increased fertilizer use (*8, 9, 48*). Production of P by mining, now ~23.5 Tg/year, is twice the background weathering rate of P released during the Holocene (*49*). Human processes are argued to have had the largest impact on the nitrogen cycle for some 2.5 billion years (*48*). Notably, the use of the Haber-Bosch process from 1913 C.E. onwards has increased the amount of reactive N in the Earth system by 120% compared to the Holocene baseline (*50*), accompanied by an increased flux of nitrogen oxides (NO_x) from the combustion of fossil fuels (*51*; Fig. 3).

These changes have stratigraphic consequences. The influx of excess reactive N and P to lakes and seas has led to seasonal oxygen deficiency, impacting local microbiota and in extreme cases increasing mortality in macrobiota (*52*). Northern Hemisphere lakes show increasingly depleted $\delta^{15}N$ values (*53, 54*), beginning ~1895 C.E. (Fig. 3B) and accelerating over the past 60 years. In Greenland ice, $\delta^{15}N$ values during Late Pleistocene glaciation show a gradual marked decline to a pre-industrial Holocene norm (mean 9.7 ‰ in GISP2 ice core; *55*), declining again and more rapidly from ~1850 C.E. with the greatest decline between 1950–1980 C.E. (*47, 56*; Fig. 3A). The main phase of increase in nitrate levels was also 1950–1980 C.E. (Fig. 3A, B), culminating in values higher than those observed for the previous 100,000 years (*57*). These are markers distinct from Holocene and Late Pleistocene background levels.

Industrial metals such as Cd, Cr, Cu, Hg, Ni, Pb and Zn have been widely and rapidly dispersed since the mid-20th century, although many show much earlier and markedly diachronous signals associated with expansion of mineral extraction and processing (*47, 58*). A great acceleration in the use of trace metals and rare earth elements (REEs) began after World War II, resulting in an increase in the amounts mined, a global pattern of dispersion in the environment, and novel stoichiometric ratios. Metals, or their derivatives, are spread through inadequate processing, a lack of recycling and reuse, or loss during everyday use. For example, platinum, rhodium and palladium lost from automotive catalytic converters accumulate preferentially in soils adjacent to highways (*59*).

Radiogenic signatures and radionuclides in sediments and ice

Potentially the most widespread and globally synchronous anthropogenic event is provided by the fallout from nuclear weapons testing. The start of the Anthropocene may thus be defined by a Global Standard Stratigraphic Age (GSSA) coinciding with detonation of the Trinity atomic device at Alamogordo, New Mexico on July 16, 1945 C.E. (*10*). But, fallout from 1945–1951 C.E. involved fission ("atomic") devices with only localized deposition of radionuclides. Fallout from thermonuclear weapon tests that began in 1952 C.E. and peaked in 1961−1962 C.E. left a clear and global signature, concentrated in the mid-latitudes and maximal in the Northern Hemisphere where most testing occurred (*47, 60, 61*; Fig. 4B). Useful potential markers include excess ^{14}C, an isotope common in nature, and ^{239}Pu, a naturally rare isotope. The Holocene segment of the IntCal13 $\Delta^{14}C$ curve, corrected for radiogenic decay ($F^{14}C$), shows past natural fluctuations and a linear normalized decrease from 1.2 to approximately 1.0

related to changes in ^{14}C production rate and global carbon cycling (*62*; Fig. 4A). An excess in ^{14}C forms a sharp bomb spike, starting in 1954 C.E. (*10*) and peaking in 1964 C.E. (*5*), both suggested as potential markers for the start of the Anthropocene. However, the peak is diachronous between hemispheres (*63*; Fig. 4B). ^{239}Pu, with a long half-life (24,110 years), low solubility and high particle reactivity, particularly in marine sediments, may be the most suitable radioisotope for marking the start of the Anthropocene (*61, 64*). The appearance of a ^{239}Pu fallout signature in 1951 C.E., peaking in 1963–1964 C.E. (Fig. 4B) will be identifiable in sediments and ice for the next 100,000 years (*61, 64*), decaying to a layer enriched in ^{235}U and, ultimately, stable ^{207}Pb.

Carbon cycle evidence from ice cores

Atmospheric CO_2, now above 400 ppm, is currently being emitted into the atmosphere ~100 times as fast as the most rapid emission of the past 800,000 years (*65*) and concentrations have exceeded Holocene levels since at least 1850 C.E. (Fig. 5). During the Late Pleistocene−Early Holocene, atmospheric CO_2 preserved in air bubbles within glacial ice in Antarctica showed a stepped 70 ppm rise over 6,000 years (*66, 67*); an average rise of 1ppm per ~85 years. Subsequent Holocene CO_2 concentrations remained approximately stable, a very slow rise of 260 to 285 ppm from ~9000 B.P. (Fig. 5A) being ascribed to early human agriculture by some (*3*), albeit controversially (*66*). CO_2 concentrations change from a slightly decreasing trend from ~11,000−8,000 B.P. to slight rising trend, commencing about 7,000 years ago (Fig. 5A). Thus, putative anthropogenic impact on atmospheric CO_2 at this time was both gradual and much less than subsequent changes over the last 200 years. The 8,200 and 4,200 year events proposed to mark the Mid- and Late Holocene Sub-epochs, respectively (*13*), show no major change in CO_2 concentrations. In sharp contrast, modern rates of atmospheric C emission (~9 Pg/year) are probably the highest of the Cenozoic Era (the last 65 Ma), likely surpassing even those of the Paleocene-Eocene thermal maximum (*68*).

The Antarctic ice core record shows steady enrichment in $\delta^{13}C$ values from Late Pleistocene to Mid-Holocene time (*66, 67*), reflecting carbon uptake by the terrestrial biosphere and carbon release from oceans (*66*; Fig. 5A), but shows no changes at the proposed Mid- and Late Holocene Sub-epoch boundaries. The Antarctic ice record shows approximately constant CO_2 and $\delta^{13}C$ values continuing from 1200−1600 C.E. (*69*; Fig. 5B). A short-lived dip at ~1610 C.E. of about 10 ppm in the CO_2 curve, and synchronous minor enrichment in $\delta^{13}C$, has been proposed as a marker for the start of the Anthropocene (*5*), though these fluctuations do not exceed natural Holocene variability (*70*; Fig. 5A). The striking change in atmospheric CO_2 concentrations is the ~120 ppm increase since ~1850 C.E. (*69*; Fig. 5B, C) rising at ~ 2 ppm/year over the past 50 years, 120 times faster than that at the start of the Holocene. This coincides with a steep fall (>2 ‰) of the $\delta^{13}C$ atmospheric CO_2 to values ~8.5 ‰ (*69*; Fig. 5C), due to an increase in ^{12}C from burning fossil hydrocarbons. This isotopic signature also forms part of the permanent record because it is inscribed in archives such as tree-rings, limestones and calcareous fossils.

Ice core records show atmospheric methane (CH_4) concentrations range from 590−760 ppb through much of the Holocene (*71-75*) up to 1700 C.E. Then, there is unprecedented increase to 1700 ppb by 2004 C.E. (*72*), some 900 ppb higher than recorded in Antarctic ice core at any time in the last 800,000 years (*76*), rising above Mid- to Late Pleistocene and

Holocene maxima by ~1875 C.E. (Fig. 5D). The $\delta^{13}C$ curve for CH_4 shows a marked decrease of ~1.5 ‰ from ~1500−1700 C.E., perhaps a response to reduced biomass burning (*72*) and subsequent abrupt rise from ~1875 C.E. to present of ~2.5 ‰ reflecting increasing pyrogenic emissions.

Climate change and rates of sea level change since the end of the last Ice Age

The proposed subdivision of the Holocene Epoch into sub-epochs (described above) reflects proxy signals for climate change (*13*). Greenland ice cores show abrupt, brief cooling events, expressed as decreases in $\delta^{18}O$ values, at 11,400, 9,300 and 8,200 B.P. (*77*; Fig. 6A), the latter proposed to define the start of the Mid-Holocene (*13*). These events are less apparent in equivalent Antarctic ice cores (*78*; Fig. 6A). A 4,200 B.P. climate shift, proposed to mark the start of the Late Holocene (*13*), is not expressed in these curves. The overall trend during the Mid- to Late Holocene is of gradual cooling (Fig. 6B), which culminated in the Little Ice Age from 1250−1800 C.E. (Fig. 6C). The cooling followed orbitally-related insolation decline, with small fluctuations representing changes in solar intensity, controlled by modulators such as the 208-year Suess cycle (*79*). Given that the orbital trend is continuing, the Earth should still be cooling. However, increased anthropogenic emissions of greenhouse gases have instead caused the planet to warm abnormally fast, over-riding the orbitally-induced climate cycle.

The shift to warming (*80, 81*; Fig. 6C) is first indicated by a slight change to less negative $\delta^{18}O$ in Greenland ice from ~1900 C.E. (Fig. 6A). This shift is well outside the declining natural envelope of temperature change for the past 1400 years (Fig. 6C), mainly due to greenhouse gases released from burning of fossil fuels and deforestation (*79, 81, 82*). Average global temperature increase of 0.6−0.9°C between 1906 and 2005 C.E., with a doubling of the rate of warming in the last 50 years (*83*), is beginning to exceed Holocene natural variability (Figs. 6B, C) in the Northern Hemisphere, and is already above Holocene maxima in the tropics and Southern Hemisphere. The change in $\delta^{18}O$ since 1900 C.E. in Greenland ice cores (Fig. 6A), is of smaller magnitude than that of the 8,200 B.P. cooling event marking the base of the Middle Holocene, but larger than that at the base of the Upper Holocene.

Average global sea levels are currently higher than at any point within the last ~115,000 years (*84*), since the termination of the last interglacial of the Pleistocene Epoch. The physical expression of sea-level change in the geological record is the displacement of sedimentary facies, for which the rate of change of sea-level relative to rates of sediment accumulation and subsidence due to compaction is crucial. For example, rapid sea level rise can cause delta tops to flood, producing sharp transitions into overlying relatively deep marine and anoxic muds, marking a flooding surface. By the time of peak sea-level the rate of rise is slower and fluvial systems can resupply sediment to re-establish deltas as progradational successions building up and out from the coast.

Very high rates of sea-level change (> 40 mm/year) occurred at about 14,000−14,300 B.P. during the Bølling warming event, with rapid ice sheet disintegration during the transition between the last glacial phase and the current interglacial phase (*85*). The magnitude of the rate of rise caused widespread inundation of coastal areas and sedimentary facies back-stepped (retrograded landwards).

The last 7,000 years of the Holocene Epoch, when ice volumes stabilized near present-day values, provides the baseline for discussion of anthropogenic contributions. Relative sea-level records indicate that from ~7,000 to 3,000 years ago, global mean sea level rose ~2 to 3 m to near present-day levels (*84*). Based on local sea-level records spanning the last 2000 years, there is medium confidence that fluctuations in global mean sea level during this interval have not exceeded ~0.25 m on time scales of a few hundred years. As a consequence, coastlines have been more or less fixed and sediment accumulation within beaches, tidal flats and deltas has been progradational.

The most robust signal captured in salt marsh records from both Northern and Southern hemispheres supports a transition from relatively low rates of change during the Late Holocene (<1 mm/year) to modern rates of 3.2 ± 0.4 mm/year from 1993−2010 C.E. (*84*). By combining paleo sea-level records with tide gauge records at the same localities, it is clear that sea level began to rise above the Late Holocene background rate between 1905 and 1945 C.E. (*86*); if continued, this will lead towards a return to dominantly retrogradational shifts in sedimentary facies along coastal zones. But, reconstructions from the Atlantic coast of the USA suggest the rising sea-level rate is not linear (*87*). A rate of rise of 0.06−0.39 mm/year during the 18th century shows a change from 1827−1860 C.E. with a subsequent late 19th century rate of 1.22−1.53 mm/year and a secondary and less pronounced change in 1924−1943 C. E., with resultant rise of 1.9−2.22 mm/year (*87*). The timing of the inflections in this rising sea-level curve matches, with an approximate decade delay, the stepped changes in CO_2 concentrations (Fig. 5c).

Compared to other stratigraphic changes described above, the climate and sea-level signals of the Anthropocene are not yet as strongly expressed, in part because they reflect the combined effects of fast and slow climate feedback mechanisms. However, given that anthropogenic forcing is clearly driving these changes, they are likely to exceed the envelope of Quaternary, and not just Holocene, baseline conditions (*79*). Projections of continued warming due to greenhouse gases, even with reduction below current emissions levels, suggest that by 2070 Earth will be at its hottest since modern humans evolved.

Changes in global average surface temperature or rise in sea level are manifestations of changes in the surface energy balance. Perhaps a more fundamental measure of human perturbation of the climate system is the human-driven change to the planetary energy balance at the Earth's surface, as measured by change in radiative forcing. Human activities, primarily the burning of fossil hydrocarbons, have increased the radiative forcing by 2.29 (1.13−3.33) W m^{-2} relative to 1750 C.E., with a more rapid increase since 1970 C.E. than during prior decades. Overwhelming the natural changes in radiative forcing during the Late Holocene (solar irradiance and volcanic aerosols), estimated to be 0.05 (0.00−0.10) W m^{-2} (*82*), the anthropogenic energy imbalance is poised to amplify stratigraphic signals associated with warming and sea-level rise.

Biotic change as an indicator of the Anthropocene

Most Phanerozoic time intervals are defined using either first or last appearance of key fossils (*29*). Evolution/extinction rates are mostly too slow and diachronous to provide an obvious biological marker for the start of the Anthropocene, but important biotic change has clearly taken place recently (*88*). Although Earth still retains most of the species that were present at

the start of the Holocene, even conservative extinction rates are far above background (Fig. 7A) since 1500 C.E., with a notable increase from the 19th century onwards (*89*; Fig. 7B). Current trends of habitat loss and over-exploitation, if maintained, would push the Earth into the sixth mass extinction event (with ~75% of species extinct) in the next few centuries (*90*), a process likely already underway (*89*).

Irrespective of the number of extinctions, species assemblages and relative abundances have altered worldwide. This is especially true in recent decades due to geologically unprecedented trans-global species invasions, and biological assemblage changes associated with agriculture on land, and fishing in the sea (*91*). The terrestrial biosphere saw a dramatic modification from 1700 C.E., when almost 50% of the global ice-free land area was wild and only ~5% was intensively used by humans, to 2000 C.E. when the respective figures were 25% and 55% (*92*). The paleontological expression of these assemblages will markedly differ from the typical Holocene fossil record as clearly recognizable, novel biostratigraphic zones (*93*) and the new assemblages of species have already permanently reconfigured Earth's biological trajectory. These biotic changes are not synchronous, but they accelerated after 1500 C.E. on land (*94*), and in the seas affecting both micro- and macrobiota (*52*).

The case for a new epoch

The stratigraphic signatures described above (Fig. 1) are either entirely novel with respect to those found in the Holocene and pre-existing epochs, or quantitatively outside the range of variation compared to those evident for Holocene subdivisions. Furthermore, most proximate forcings of these signatures are currently accelerating. These unique attributes of the recently-formed geological record support the formalization of the Anthropocene as a stratigraphic entity equivalent to other formally defined geological epochs. The boundary should therefore be placed following procedures of the International Commission on Stratigraphy.

If such formalization is to be achieved, however, further work is required. Firstly, it needs to be determined how the Anthropocene is to be defined, whether by GSSA (calendar age) or GSSP (reference point in a stratal section; *10*), or combination of both. Whichever is ultimately chosen, location and comparative analysis of candidate stratotype sections is necessary, not least to explore how effectively any chosen levels may be traced and correlated within stratal archives. This is linked to the question of when exactly the Anthropocene may be determined to begin. Although the analysis above is more consistent with a mid-20th century beginning, within that interval a number of options have already been suggested, ranging from 1945 to 1964 C.E. (*5, 10*). There is also the question, still under debate, of whether it is helpful to formalize the Anthropocene, or better to leave it as an informal, albeit solidly founded geological time term, as are currently the Precambrian and the Tertiary (*95*). This is a complex and as yet unresolved question, in part because quite unlike other subdivisions of geological time terms the implications of formalizing the Anthropocene reach well beyond the geological community. Indeed, not only would this represent the first instance of a new epoch having been witnessed first-hand by advanced human societies, it would be one stemming from the consequences of their own doing.

References:

1. W. Steffen *et al.,* The Anthropocene: conceptual and historical perspectives. *Philos. Trans. R. Soc. London Ser. A* **369,** 842–867 (2011).
2. A. Malm, A. Hornborg, The geology of mankind? A critique of the Anthropocene narrative. *The Anthropocene Review* **1(1)**, 62–69 (2014).
3. W. F. Ruddiman, The Anthropogenic Greenhouse Era began thousands of Years Ago. *Clim. Change* **61**, 261–293 (2003).
4. W. F. Ruddiman, Anthropocene. *Annu. Rev. Earth Planet. Sci.* **41**, 45–68 (2013).
5. S. L. Lewis, M. A. Maslin, Defining the Anthropocene. *Nature* **519**, 171–180 (2015).
6. P. J. Crutzen, Geology of Mankind. *Nature* **415**, 23 (2002).
7. J. Zalasiewicz *et al*., Are we now living in the Anthropocene? *Geol. Soc. Am. Today* **18**, 4–8 (2008).
8. W. Steffen *et al*., The Anthropocene: are humans now overwhelming the great forces of Nature? *Ambio* **36**, 614–621 (2007).
9. W. Steffen *et al*., The trajectory of the Anthropocene: The Great Acceleration. *The Anthropocene Review* **2(1)**, 81–98 (2015).
10. J. Zalasiewicz *et al*., When did the Anthropocene begin? A mid-twentieth century boundary level is stratigraphically optimal. *Quaternary International* **383**, 196–203 (2015).
11. B. Pillans, P. Gibbard, The Quaternary Period. In: *The Geologic Time Scale*, F. M. Gradstein et al. Eds. (Elsevier B.V., 2012) 979–1010.
12. J. Remane *et al*., Guidelines for the establishment of global chronostratigraphic standards by the International Commission on Stratigraphy (ICS). *Episodes* **19**, 77–81 (1996).
13. M. Walker *et al*., Formal subdivision of the Holocene Series/Epoch: a Discussion Paper by a Working Group of INTIMATE (Integration of ice-core, marine and terrestrial records) and the Subcommission on Quaternary Stratigraphy (International Commission on Stratigraphy). *J. Quat. Sci.* **27**, 649–659 (2012).
14. I. McDougall *et al*., Stratigraphic placement and age of modern humans from Kibish, Ethiopia. *Nature* **433**, 733–736 (2005).
15. HYDE (History Database of the Global Environment) database. Netherlands Environmental Assessment Agency (2013). http://themasites.pbl.nl/tridion/en/themasites/hyde/basicdrivingfactors/population/index-2.html [Accessed 15th February, 2013].
16. K. Klein Goldewijk *et al*., Long-term dynamic modeling of global population and built-up area in a spatially explicit way: HYDE 3.1. *The Holocene* **20(4)**, 565–573 (2010).
17. A. D. Barnosky *et al*., Prelude to the Anthropocene: Two new North American Land Mammal Ages (NALMAs). *The Anthropocene Review* **1,** 225–242 (2014).
18. C. N. Waters *et al*., A stratigraphical basis for the Anthropocene? In *A Stratigraphical Basis for the Anthropocene,* C. N. Waters *et al*. Eds. (Geol. Soc., London, 2014), 1–21.

19. J. R. Ford *et al*., An assessment of lithostratigraphy for anthropogenic deposits. In: *A Stratigraphical Basis for the Anthropocene,* C. N. Waters et al. Eds. (Geol. Soc., London, 2014), 55–89.

20. J. Zalasiewicz *et al*., The mineral signature of the Anthropocene. In *A Stratigraphical Basis for the Anthropocene,* C. N. Waters *et al*. Eds. (Geol. Soc., London, 2014), 109–117.

21. M. Edgeworth *et al*., Diachronous beginnings of the Anthropocene: The lower bounding surface of anthropogenic deposits *The Anthropocene Review* **2(1)**, 33–58 (2015).

22. J. Zalasiewicz *et al*., Anthropocene. In *Origins* O. Seberg, D. A. Harper Eds. (CUP, 2016).

23. US Geological Survey in *Historical Statistics for Mineral and Material Commodities in the United States*, T. D. Kelly, G. R. Matos Eds. (US Geological Survey Data Series, **140** 2010).

24. Plastics Europe (2013) Available: www.plasticseurope.de/cust/documentrequest.aspx?DocID559179.

25. P.L. Corcoran. Benthic plastic debris in marine and fresh water environments. *Environ. Sci.: Processes Impacts*, 17, 1363-1369 (2015).

26. R. C. Thompson *et al*., Lost at sea: where is all the plastic? *Science* **304**, 838 (2004).

27. J. R. Jambeck *et al*., Plastic waste inputs from land into the ocean. *Science* **347**, 768–771 (2015).

28. J. Zalasiewicz *et al*., The technofossil record of humans. *Anthropocene Review* **1**, 34–43 (2013),

29. A. G. Smith *et al*., GSSPs, global stratigraphy and correlation. In: *Strata and Time: Probing the Gaps in Our Understanding,* D. G. Smith *et al*. Eds. (Geol. Soc., London, 2014), 37–67.

30. T. Novakov *et al*., Large historical changes of fossil-fuel black carbon aerosols. *Geophys. Res. Lett.* **30(6)** 1324, 57-1–57-4 (2003).

31. F. Oldfield, Can the magnetic signatures from inorganic fly ash be used to mark the onset of the Anthropocene? *Anthropocene Review* **2(1)**, 3–13 (2014).

32. N. L. Rose, Spheroidal carbonaceous fly ash particles provide a globally synchronous stratigraphic marker for the Anthropocene. *Environ. Sci. Technol.* **49(7)**, 4155–4162 (2015).

33. G. T. Swindles *et al*., Spheroidal carbonaceous particles are a defining stratigraphic marker for the Anthropocene. *Scientific Reports* **5(10264)** (2015). doi:10.1038/srep10264.

34. M. C. Harvey *et al*., Combustion of fossil organic matter at the Cretaceous-Paleogene (K-P) boundary. *Geology* **36(5)**, 355–358 (2008).

35. R. LeB. Hooke, *et al*., Land transformation by humans: a review. *Geol. Soc. Am. Today* **22**, 4–10 (2012).

36. J. Zalasiewicz *et al*., Can an Anthropocene Series be defined and recognized?. In *A Stratigraphical Basis for the Anthropocene,* C. N. Waters *et al*. Eds. (Geol. Soc., London, 2014), 39–53.

37. J. Zalasiewicz *et al*., Human bioturbation, and the subterranean landscape of the Anthropocene. *Anthropocene,* **6***,* 3–9 (2014).

38. I. Douglas, N. Lawson, The human dimensions of geomorphological work in Britain. *J. Industrial Ecology* **4**, 9–33 (2001).

39. Ellis, E.C. 2011. Anthropogenic transformation of the terrestrial biosphere. *Proc. R. Society A*: Mathematical, Physical and Engineering Science **369**, 1010–1035.

40. A. Brown *et al*., Geomorphology of the Anthropocene: Time-transgressive discontinuities of human-induced alluviation. *Anthropocene* **1**, 3–13 (2013).

41. P. Meyfroidt, E.F. Lambin. 2011. Global Forest Transition: Prospects for an End to Deforestation. *Annu. Rev. Env. Resour*. **36**, 343–371.

42. Sidle, R.C., Ziegler, A.D., The dilemma of mountain roads. Nat. Geosci. **5**, 437–438. (2012).

43. J. P. M. Syvitski, A. Kettner, Sediment flux and the Anthropocene. *Philos. Trans. R. Soc. London Ser. A* **369**, 957–975 (2011).

44. C. K. Paull *et al*., Discordant ^{14}C-stratigraphies in upper Monterey Canyon: A signal of anthropogenic disturbance. *Mar. Geol*. **233**, 21–36 (2006).

45. C. H. Vane *et al*., Chemical signatures of the Anthropocene in the Clyde estuary, UK: sediment-hosted Pb, $^{207/206}$Pb, total petroleum hydrocarbon, polyaromatic hydrocarbon and polychlorinated biphenyl pollution records. *Philos. Trans. R. Soc. London Ser. A*., **369**, 1085–1111 (2011).

46. D. C. G Muir, N. L. Rose, Persistent organic pollutants in the sediments of Lochnagar. In: *Lochnagar: The Natural History of a Mountain Lake*, N. L. Rose Ed. (Springer, Dordrecht, 2007), 375–402.

47. J. R. Dean *et al*., Is there an isotopic signature of the Anthropocene? The Anthropocene Review **1(3),** 276–287.

48. D. E. Canfield *et al*., The evolution and future of Earth's Nitrogen Cycle. *Science* **330**, 192–196 (2010).

49. S. R. Carpenter, E. M. Bennett, Reconsideration of the planetary boundary for phosphorus. *Environ. Res. Lett*. **6**, 1–12 (2011).

50. J. N. Galloway *et al*., Transformation of the Nitrogen Cycle: Recent trends, questions, and potential solutions. *Science* **320**, 889–892 (2008).

51. E. A. Holland *et al*., Global N Cycle: Fluxes and N_2O Mixing Ratios Originating from Human Activity. Data set. Available on-line [http://www.daac.ornl.gov] from Oak Ridge National Laboratory Distributed Active Archive Center, Oak Ridge, Tennessee, U.S.A. (2005).

52. I. P. Wilkinson *et al*., Micropalaeontological signatures of the Anthropocene. In *A Stratigraphical Basis for the Anthropocene,* C. N. Waters *et al*. Eds. (Geol. Soc., London, 2014), 185–219.

53. G. W. Holtgrieve *et al*., A Coherent Signature of Anthropogenic Nitrogen Deposition to Remote Watersheds of the Northern Hemisphere. *Science* **334**, 1545–1548 (2011).

54. A. P. Wolfe *et al*., Stratigraphic expressions of the Holocene–Anthropocene transition revealed in sediments from remote lakes. *Earth. Sci. Rev.* **116**, 17–34 (2013).

55. M. G. Hastings *et al*., Glacial/interglacial changes in the isotopes of nitrate from the Greenland Ice Sheet Project 2 (GISP2) ice core. *Global Biogeochem Cy* **19**, GB4024 (2005).

56. M. G. Hastings *et al*., Anthropogenic impacts on nitrogen isotopes of ice-core nitrate. *Science* **324**, 1288 (2009).

57. E. W. Wolff, Ice Sheets and the Anthropocene. In *A Stratigraphical Basis for the Anthropocene,* C. N. Waters *et al*. Eds. (Geol. Soc., London, 2014), 255–263.

58. A. Gałuszka *et al*., Assessing the Anthropocene with geochemical methods. In *A Stratigraphical Basis for the Anthropocene,* C. N. Waters *et al*. Eds. (Geol. Soc., London, 2014), 221–238.

59. K. E. Jarvis *et al*., Temporal and Spatial Studies of Autocatalyst-Derived Platinum, Rhodium, and Palladium and Selected Vehicle-Derived Trace Elements in the Environment. *Environ. Sci. Technol*., **35(6)**, 1031–1036 (2001).

60. UNSCEAR-United Nations Scientific Committee on the Effects of Atomic Radiation *Sources and Effects of Ionizing Radiation*, (New York: United Nations, 2000).

61. C. N. Waters *et al*., Can nuclear weapons fallout mark the beginning of the Anthropocene Epoch? *B. Atom. Sci.* **71(3),** 46–57 (2015).

62. P. J. Reimer *et al*., IntCal13 and Marine13 radiocarbon age calibration curves 0-50,000 years cal BP. *Radiocarbon* **55**, 1869–1887 (2013).

63. Q. Hua *et al*., Atmospheric radiocarbon for the period 1950−2010. *Radiocarbon* **55**, 2059–2072 (2013).

64. G. J. Hancock *et al*., The release and persistence of radioactive anthropogenic nuclides. In *A Stratigraphical Basis for the Anthropocene,* C. N. Waters *et al*. Eds. (Geol. Soc., London, 2014), 265–281.

65. E.W. Wolff, Greenhouse gases in the Earth system: a palaeoclimate perspective. *Philos. Trans. Roy. Soc*. *London Ser. A*, **369**, 2133-2147 (2011).

66. J. Elsig *et al*., Stable isotope constraints on Holocene carbon cycle changes from an Antarctic ice core. *Nature* **461(7263)**, 507–510 (2009).

67. J. Schmitt *et al*., Carbon isotope constraints on the deglacial CO_2 rise from ice cores. *Science* **336**, 711–714 (2012).

68. Y. Cui *et al*. Nature Geoscience, Slow release of fossil carbon during the Palaeocene–Eocene Thermal Maximum *Nature Geoscience* **4**, 481–485 (2011).

69. M. Rubino *et al*., A revised 1000 year atmospheric $\delta^{13}C$-CO_2 record from Law Dome and South Pole, Antarctica. *J. Geophys. Res.* **118**, 8482–8499 (2013).

70. J. Zalasiewicz *et al*., Colonization of the Americas, 'Little Ice Age' climate, and bomb-produced carbon: Their role in defining the Anthropocene. *The Anthropocene Review* **2**, 117–127 (2015).

71. T. Blunier *et al*., Variations in atmospheric methane concentration during the Holocene epoch. *Nature* **374**, 46–49 (1995).

72. D. F. Ferretti *et al*., Unexpected changes to the global methane budget over the past 2000 years. *Science* **309**, 1714–1717 (2005).

73. C. MacFarling Meure *et al*., Law Dome CO_2, CH_4 and N_2O ice core records extended to 2000 years BP. *Geophys. Res. Lett.* **33**, L14810 (2006).

74. C. J. Sapart *et al*., Natural and anthropogenic variations in methane sources during the past two millennia. *Nature* **490**, 85–88 (2012).

75. L. Mitchell *et al*., Constraints on the Late Holocene anthropogenic contribution to the atmospheric methane budget. *Science* **342**, 964–966 (2013).

76. L. Loulergue *et al*., *IGBP PAGES, World Data Center for Paleoclimatology*, Data Contribution Series # 2008 - 054. NOAA/NGDC Paleoclimatology Program, Boulder CO, USA. (accessed from the Carbon Dioxide Information Analysis Center, Oak Ridge National Laboratory, U.S. Department of Energy) (2008).

77. B. M. Vinther *et al*., A synchronized dating of three Greenland ice cores throughout the Holocene. *J. Geophys. Res.* **111**, D13102 (2006).

78. T. Felis *et al*., Pronounced interannual variability in tropical South Pacific temperatures during Heinrich Stadial 1. *Nature Communications* **3**, 965. DII: 10.1038/ncomms1973 (1973).

79. C. P. Summerhayes, *Earth's Climate Evolution* (Wiley/Blackwell, 2015) 390pp.

80. PAGES 2k Consortium, Continental-scale temperature variability during the last two millennia. *Nature Geoscience* **6**, 339–346 (2013).

81. H. Wanner *et al*., Holocene climate variability and change; a data-based review. *J. Geol. Soc. London* **172**, 254–263 (2015).

82. IPCC, *Climate Change 2013: The Physical Science Basis*. Summary for Policymakers. L. Alexander *et al*. (IPCC Secretariat, Geneva, Switzerland, 2013).

83. J. R. Hansen *et al*., Global surface temperature change. *Rev. Geophys*. **48**, RG4004 (2010).

84. J. A. Church *et al*., Sea level change. In: *Climate Change 2013: The Physical Science Basis*. Contribution of Working Group I to the Fifth Assessment Report of the Intergovernmental Panel on Climate Change, T. F. Stocker *et al*., Eds. (Cambridge University Press, Cambridge, United Kingdom and New York, NY, USA, 2013), 1137–1216.

85. P. Deschamps *et al*., Ice-sheet collapse and sea-level rise at the Bølling warming 14,600 years ago. *Nature* **483**, 559–564 (2012).

86. R. Gehrels, P. L. Woodworth, When did modern rates of sea-level rise start? *Global Planet. Change* **100**, 263–277 (2013).

87. A. C. Kemp et al., Relative sea-level change in Connecticut (USA) during the last 2200yrs. *Earth Planet. Sci. Lett*. **428**, 217–229 (2015).

88. A. D. Barnosky, Palaeontological evidence for defining the Anthropocene. In *A Stratigraphical Basis for the Anthropocene,* C. N. Waters *et al*. Eds. (Geol. Soc., London, 2014), 149–165.

89. G. Ceballos *et al*., Accelerated modern human–induced species losses: Entering the sixth mass extinction. *Sci. Adv*. **1**, e1400253 (2015). doi: 10.1126/sciadv.1400253.

90. A. D. Barnosky *et al*., Has the Earth's sixth mass extinction already arrived? *Nature* **486**, 52–56 (2012).

91. M. Williams *et al*., The Anthropocene biosphere. *The Anthropocene Review* (2015). doi: 10.1177/2053019615591020.

92. E. C. Ellis *et al*., Anthropogenic transformation of the biomes. *Global Ecol. Biogeogr.* **19**, 589–606 (2010).

93. S. M. Kidwell, Biology in the Anthropocene: Challenges and insights from young fossil records. *Proc. Natl. Acad. Sci.* **112**, 4922–4929 (2015).

94. J. R. McNeill, Biological Exchanges in World History. In: J. Bentley, Ed., *The Oxford Handbook of World History* (Oxford: Oxford University Press, 2011) 325–342.

95. W. F. Ruddiman *et al*. Defining the epoch we live in: Is a formally designated "Anthropocene" a good idea? *Science* **348**, 38–39 (2015).

Acknowledgments: CW and ME publish with the permission of the Executive Director, British Geological Survey, Natural Environment Research Council, the former funded with the support of the British Geological Survey's Engineering Geology science program. We thank three referees, along with I. Fairchild, I. Hajdas and S. Price for their comments. This paper is a contribution of the Anthropocene Working Group (AWG), part of the Subcommission on Quaternary Stratigraphy of the International Commission on Stratigraphy (ICS). The AWG receives no direct funding to carry out its research and the authors declare no competing financial interests.

Figures

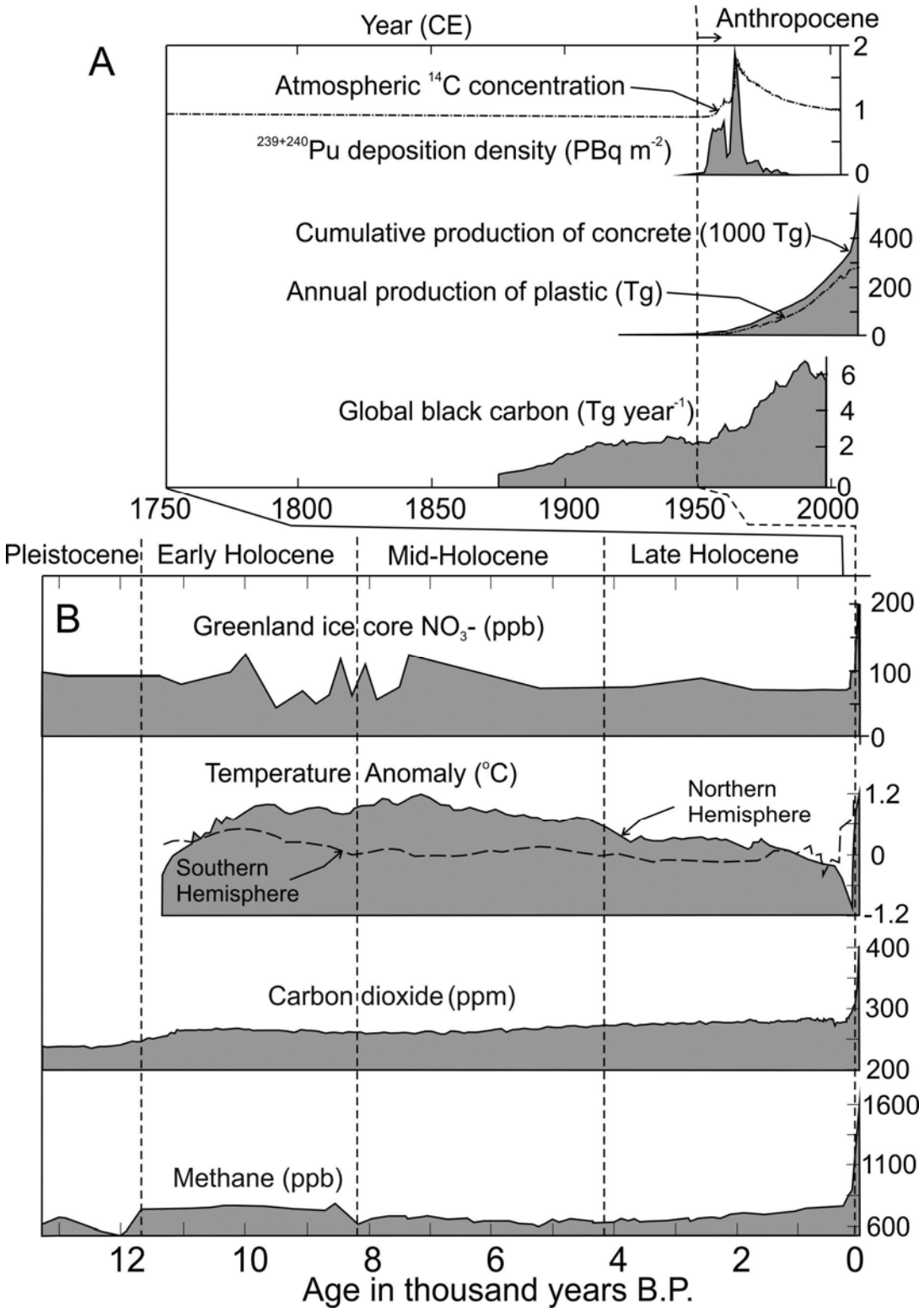

Fig. 1. Summary of the magnitude of key markers of anthropogenic change indicative of the Anthropocene. (A) Novel markers, such as concrete, plastics, global black carbon and plutonium (Pu) fallout compared with

excess and radiocarbon (^{14}C); (B) long-ranging signals such as nitrates (NO_3-), CO_2, CH_4 and global temperatures, which remain at relatively low values prior to 1950, rapidly rise during the mid-20th century and, by late 20th century, exceed Holocene ranges.

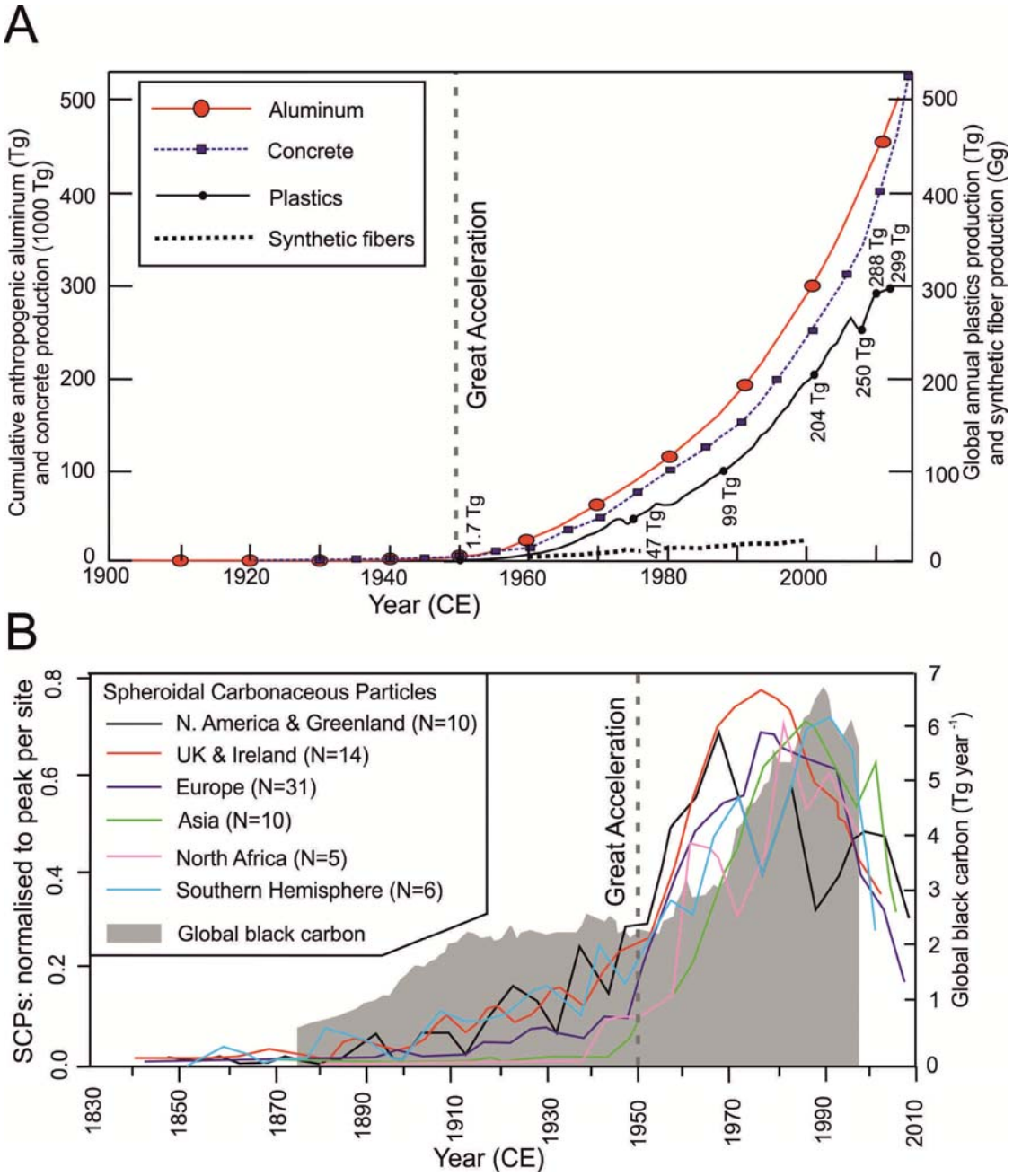

Fig. 2. The production of selected new anthropogenic materials. (A) Cumulative growth of manufactured aluminum in the surface environment (adapted from data in *23*, assuming a recycling rate of 50%). Cumulative growth of production of concrete, assuming most cement goes into concrete and that ~15% of average concrete mass is cement (from *22*, derived from United States Geological Survey global cement production statistics). Annual growth of plastics production (from *24*) and synthetic fibers production (Gg/year) from *26*; (B) Global mid-20th century rise and late-20th century spike in spheroidal carbonaceous particles normalized to the peak value in each lake core (modified from *32*) and global black carbon for available annual fossil fuel consumption data of 1875–1999 C.E. (*30*).

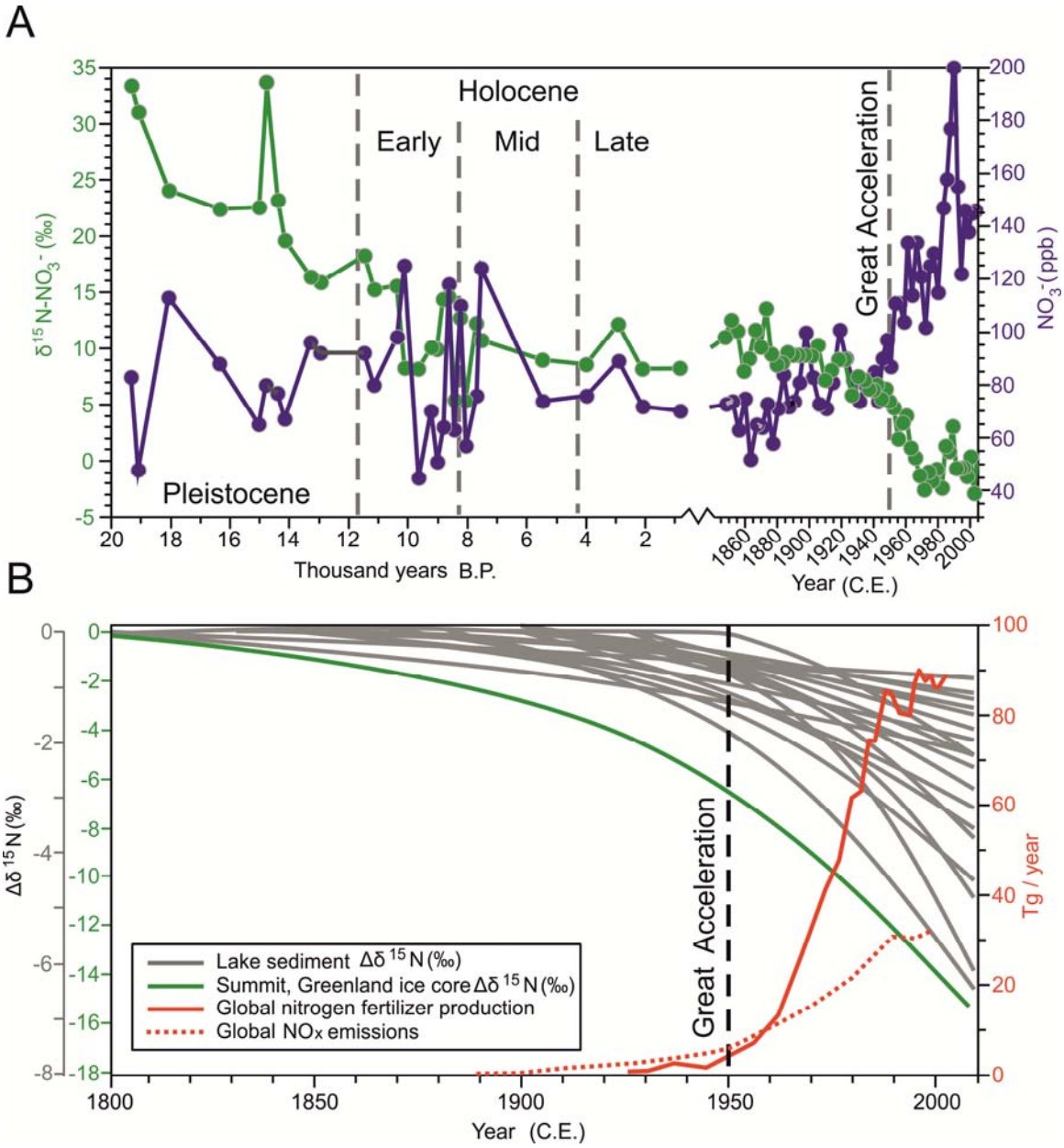

Fig. 3. Perturbations of the nitrogen cycle since the start the Late Pleistocene. (A) Co-evolution of ice core NO_3^- (blue) and $\delta^{15}N\text{-}NO_3^-$ (green) from the Late Pleistocene to the present, obtained by splicing data from two cores from Summit, Greenland (72.5˚N, 38.4˚W, 3200 m a.s.l.) (*55-57*). (B) Power functions fitted to lake-sediment (gray lines, representing 25 remote Northern Hemisphere sites) and ice core (green) $\delta^{15}N$ data, expressed as departures (*i.e.*, $\Delta\delta^{15}N$) relative to pre-industrial baseline values (*53, 54*). These isotopic trends are shown alongside annual rates of reactive N production from agricultural fertilizer (solid red line) and NO_x emissions from fossil fuel combustion (dashed red) (*51*).

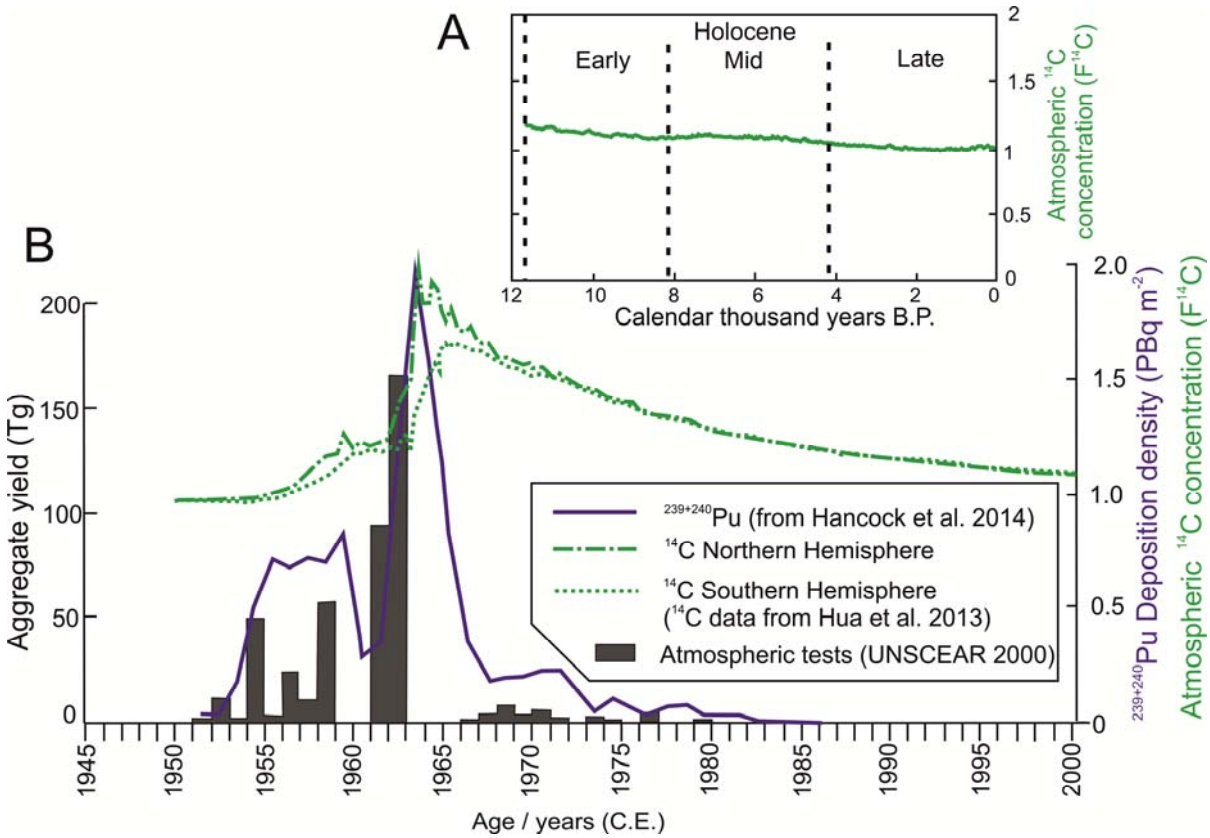

Fig. 4. Radiogenic fallout signals as a marker for the Anthropocene. (A) Age-corrected atmospheric ^{14}C concentration ($F^{14}C$) based on IntCal13 curve prior to nuclear testing (*62*); (B) concentration of ^{14}C ($F^{14}C$) measured in atmosphere (*63*) and $^{239+240}Pu$ (*64*) radiogenic fallout from nuclear weapons testing plotted against annual aggregate atmospheric weapons test yields (*60*).

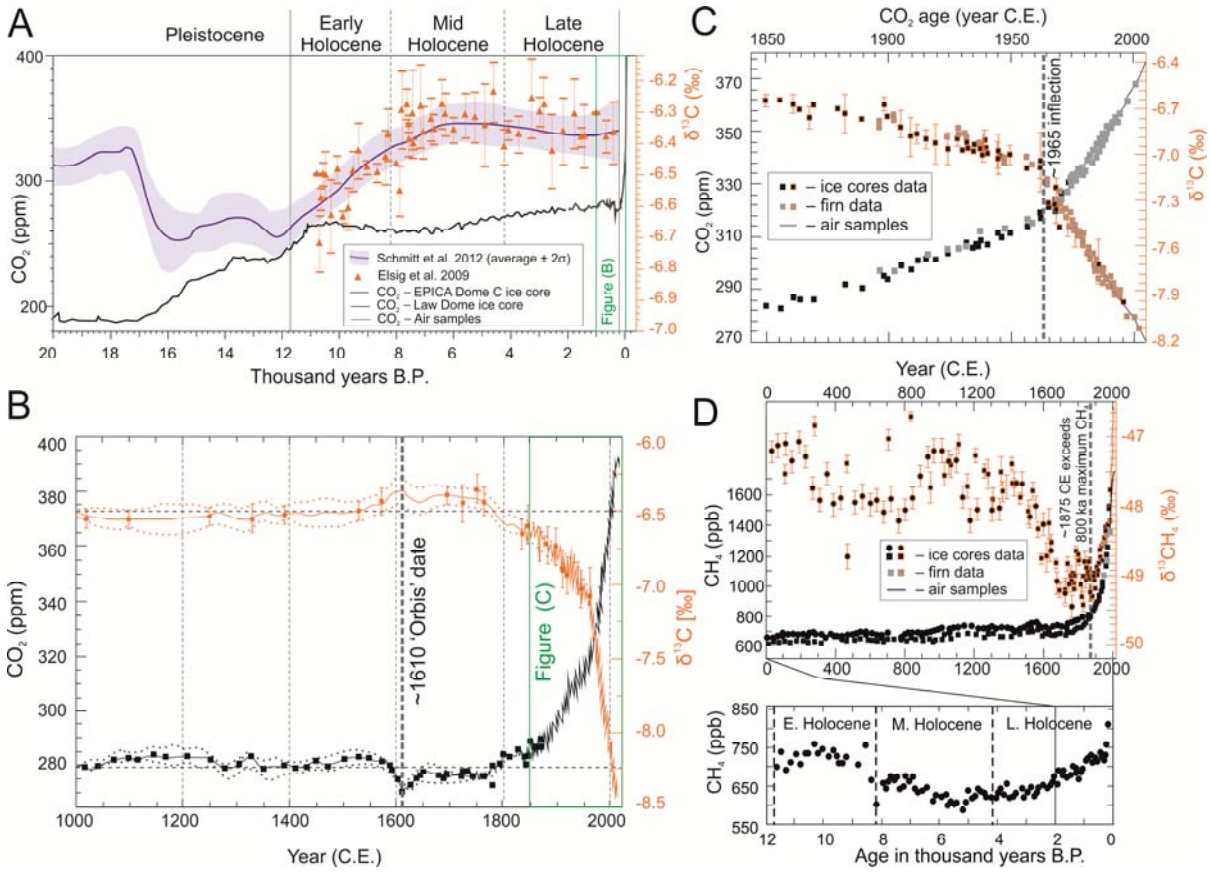

Fig. 5. Perturbations of the carbon cycle evidenced by glaciochemical CO_2 and CH_4 concentrations and carbon isotopic ratios. (A) Atmospheric CO_2 from the Antarctic Law Dome and EPICA Dome C ice cores combined with data from observed measurements (sourced from *69* and references therein), and $\delta^{13}C$ from atmospheric CO_2 (*66*, *67*); (B) CO_2 concentration and $\delta^{13}C$ from atmospheric CO_2 from the Law Dome ice cores (from *69*) showing a 10 ppm dip in CO_2 recognized as the 'Orbis' event (*5*); (C) CO_2 concentration and $\delta^{13}C$ from atmospheric CO_2 from the Law Dome ice core, firn data and air samples (from *69*) showing inflections at ~1965 C.E.; (D) Antarctic (shown as squares) and Greenland (shown as circles) ice core and firn records for CH_4 concentration and $\delta^{13}C$ for the last two millennia (*72-75*) and for Greenland ice core throughout the Holocene (*71*).

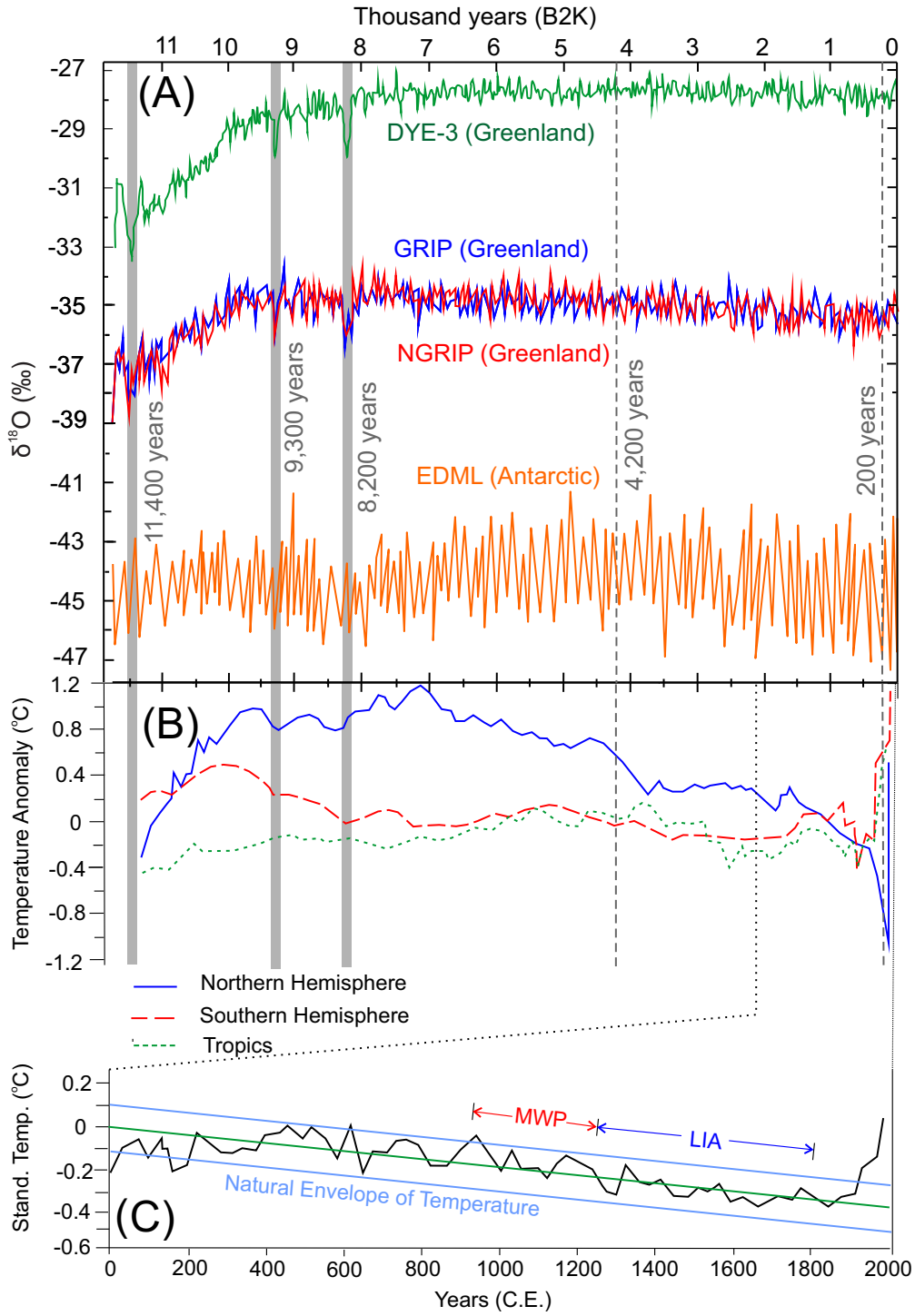

Fig. 6. Climate variations during the Holocene indicated by oxygen isotopic ratios and modelled temperature variations. (A) Holocene profiles of $\delta^{18}O$ for the three Greenland ice cores with three short-duration cooling events indicated by shading (*77*) and comparison with Antarctic EPICA (EDML) ice core (*78*); (B) Temperature reconstructions for the Holocene and global temperatures for the last 2000 years (*81*); (C) standardized global mean temperature for the last 2000 years, represented by 30 year means (*80, 81*), showing natural temperature envelope for the past 2000 years (based on *79*), including the LIA- Little Ice Age; and MWP- Medieval Warm Period (Medieval Climatic Anomaly) of the Northern Hemisphere.

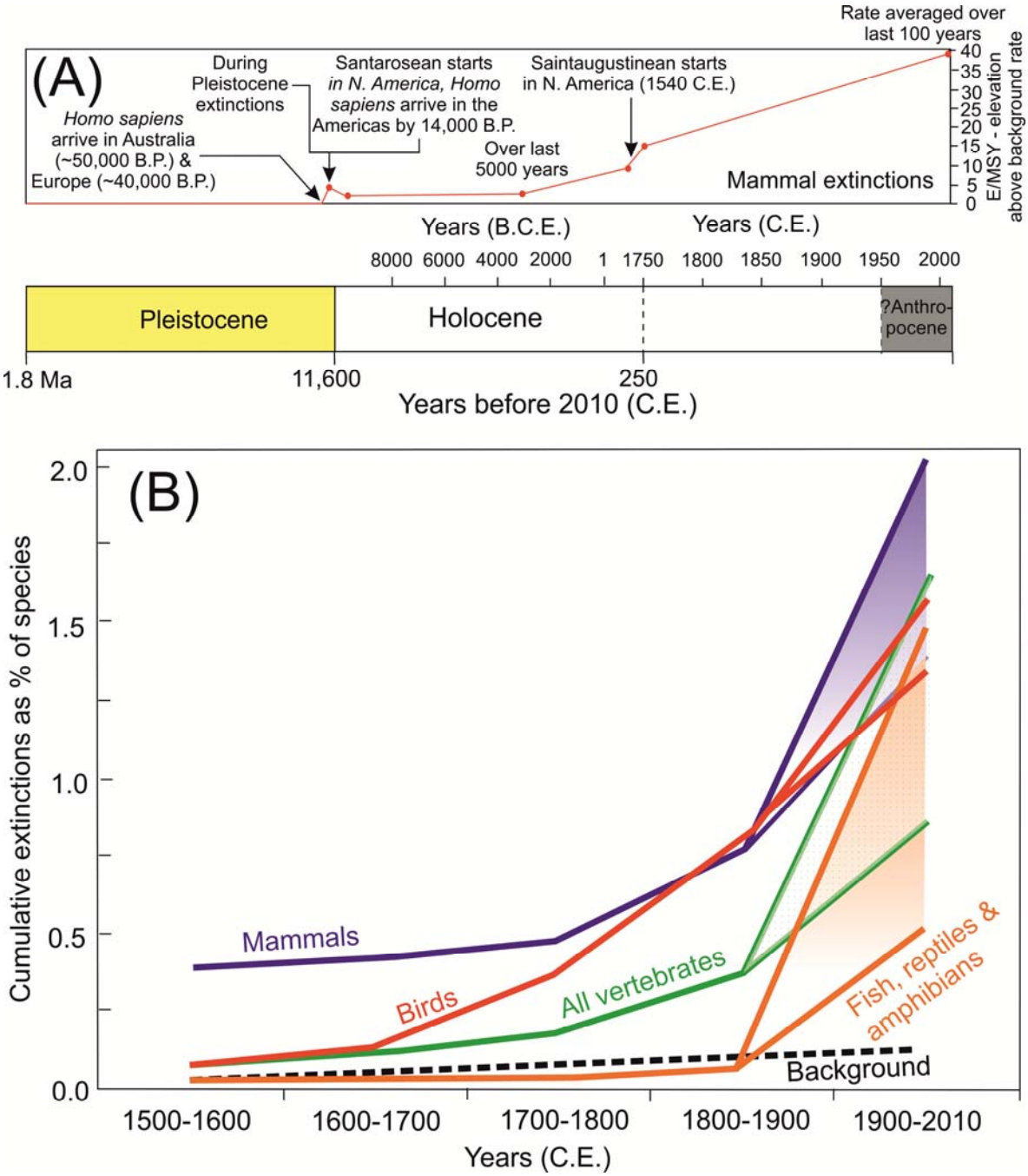

Fig. 7. Increased rates of vertebrate extinctions. (A) The approximate rise in mammal extinction rates when calculated over varying time intervals as extended backwards from the 2010 C.E. Lines indicate the amount by which extinction rates exceed 1.8 extinctions per million species-years (E/MSY) (see *89*; sourced from *22*): (B) Cumulative vertebrate species extinctions as a percentage of total species with ranges between conservative rates (includes extinctions, extinctions in the wild and possible extinctions) and lower highly conservative rates (verified extinctions only). A background rate of 2.0 E/MSY is shown for comparison (after *89*).